

Space-Charge-Limited Conduction in Vacuum-Deposited PVDF Films

S. P. BODHANE, V. S. SHIRODKAR

Solid State Electronics Lab., Department of Physics, The Institute of Science, Mumbai 400 032, India

Received 13 March 1998; accepted 25 March 1999

ABSTRACT: Current–voltage characteristics of poly(vinylidene fluoride) (PVDF) films fabricated on glass substrates by thermal evaporation technique in the metal–polymer–metal sandwich configuration were studied. The vacuum-deposited PVDF films were predominantly of α form. However, when subjected to high-voltage, short-duration singular pulse, it possibly resulted in mixed $\alpha + \beta$ form. The I – V curves of such films display the low-field ohmic region and the high-field square-law region. The current versus thickness curves in the square-law region and the transition voltage, V_{tr} , versus thickness curves indicate the conduction process to be space–charge-limited. The analyses of the current–voltage characteristics indicated the presence of uniformly distributed high-trapping carrier densities on the order of $10^{24} \text{ m}^{-3} \text{ eV}^{-1}$ with average activation energy of 0.263 eV. © 1999 John Wiley & Sons, Inc. *J Appl Polym Sci* 74: 1347–1354, 1999

Key words: polymer; PVDF; SCLC; vacuum deposition; thin film

INTRODUCTION

The discovery of strong piezoelectricity in poly(vinylidene fluoride) (PVDF) has drawn considerable research interest of both scientists and technologists. PVDF exists in different crystalline forms named as α , β , γ , and δ .^{1–3} The β form has molecules in planar–zigzag configuration. Its unit cell is orthorhombic with space group Cm2m. There are two polymer chains per unit cell and the monomer units are rigid dipoles of moment $7 \times 10^{-30} \text{ C m}$. Thus, a single crystal will clearly be piezo- and pyroelectric.⁴

The α phase is monoclinic with space group P2₁/C. Each unit cell again contains two molecular chains that are in the *trans–gauche–trans–gauche'* configuration. In this configuration, the dipole moments of alternate monomer units along

the chain are oriented at different angles and the overall crystal is nonpolar.

Oriented β -phase samples can be obtained by stretching melt-crystallized samples to about four times their original length, at about 50°C, whereas the α phase can be obtained by crystallization from the melt. There are indications that an electric field can flip one of the chains on the unit cell of α phase over to a new polar form and that at higher electric fields the configuration of the molecules can be changed from *trans–gauche–trans–gauche'* to planar–zigzag.^{4,5} The β phase, which is a polar form, is known to be mainly responsible for piezoelectric activity in PVDF. However, α phase, which is nonpolar, is also known to give rise to a large piezoelectric effect.^{6–8}

For the device applications, it is essential to identify the type of conduction mechanism prevalent in these films. A good amount of work on electrical conduction in polymeric material was reported by many researchers.^{9–12} However, most of the electrical measurements carried out on the

Correspondence to: V. S. Shirodkar.

Journal of Applied Polymer Science, Vol. 74, 1347–1354 (1999)

© 1999 John Wiley & Sons, Inc.

CCC 0021-8995/99/061347-08

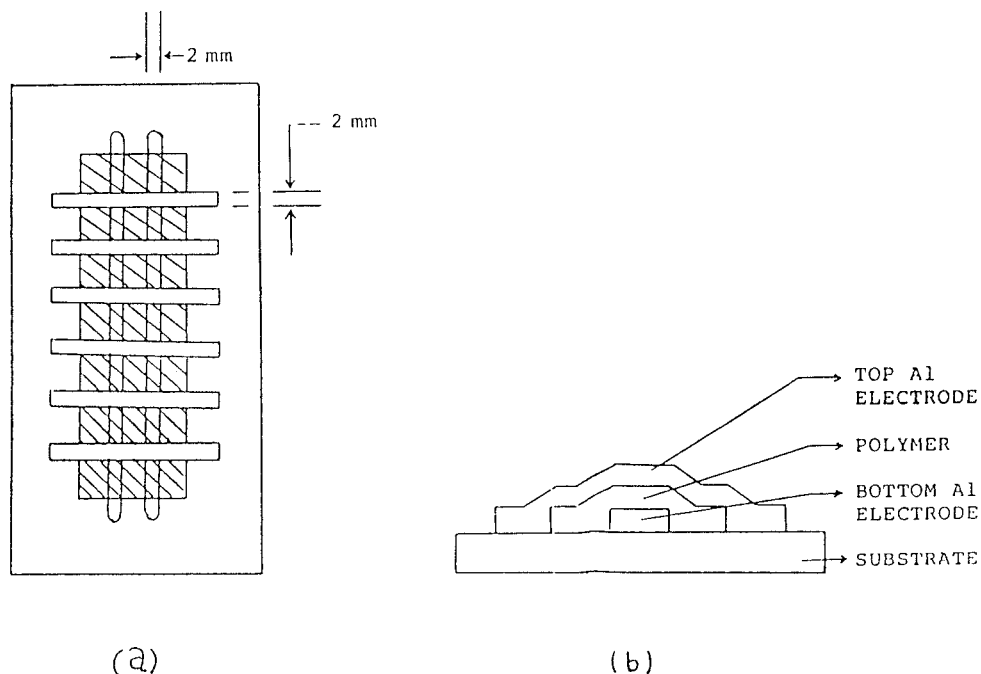


Figure 1 MPM devices: (a) planar structure, and (b) cross section.

PVDF films were solution cast and in the thickness range of 10–80 μm and biaxially or uniaxially stretched. For many device applications, a patterning of films is required which can be conveniently carried out during film fabrication by depositing films through suitable masks. It was shown¹³ that it is possible to grow good-quality PVDF films, in the form of metal–polymer–metal (MPM) structure on glass substrates using the vacuum evaporation technique.

To the best of our knowledge, no attempt was made to study the dc conduction in PVDF films, with thickness $< 1 \mu\text{m}$, cast by using vacuum evaporation technique. In the present study, therefore, we report on a dc conduction mechanism in vacuum-deposited PVDF films having thicknesses $< 0.25 \mu\text{m}$.

EXPERIMENTAL

The PVDF samples used in the present study were fabricated on thoroughly cleaned microscope glass slides with dimensions of $75 \times 25 \text{ mm}$. The PVDF powder used for evaporation was supplied by Aldrich Chemical Co., Inc. (Milwaukee, WI) and possessed an average molecular weight of 5×10^5 a.m.u.

The metal–polymer–metal devices were fabricated by sequential vacuum evaporation of aluminum, polymer, and again aluminum by using appropriate masks. The entire evaporation sequence was completed without breaking vacuum at any stage. One evaporation cycle could provide 12 MPM devices on a single substrate (Fig. 1) fabricated essentially under identical deposition conditions. The thickness of aluminum was kept at at least $0.6 \mu\text{m}$ to ensure good electrical contacts and also to prevent migration of sodium ions at elevated temperatures from the glass substrate into the active area of the devices.

All the electrical measurements on MPM devices were carried out in a vacuum cryostat, which could be evacuated to 10^{-2} Torr during the measurements. The voltage–current measurements were made using Keithley electrometer model 610C and Keithley nanovoltmeter Model 181. The films used to obtain IR spectra were fabricated by depositing PVDF vapors simultaneously on a KBr pellet and the substrate held close to one another in a vacuum chamber during the evaporation. The details are given in the previous article.¹³

RESULTS AND DISCUSSION

As mentioned before, the PVDF film may exist in α , β , $\alpha + \beta$, or γ form. It is therefore essential to

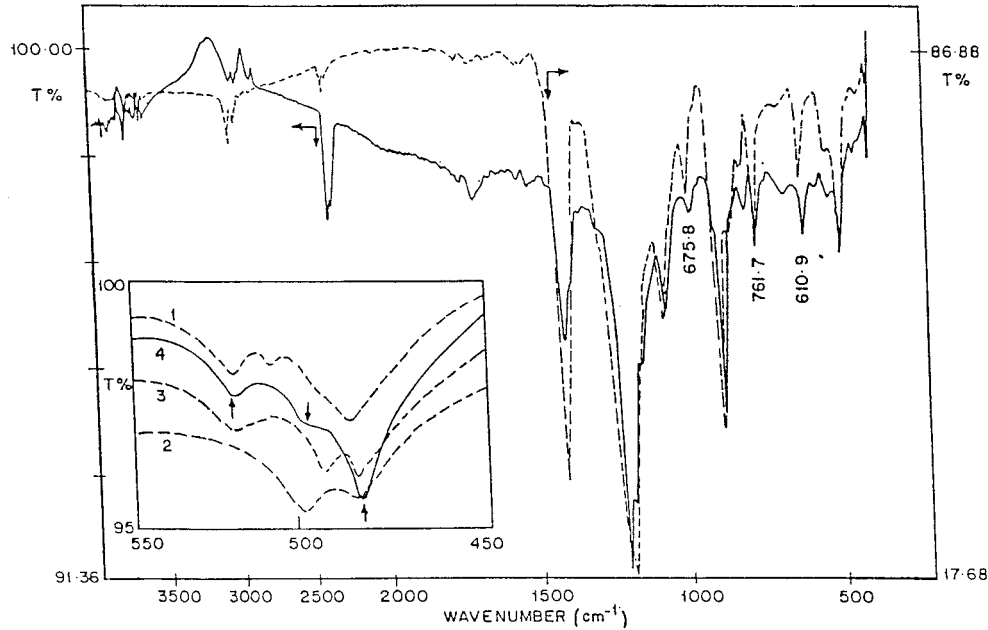


Figure 2 IR spectra of (—) thermally evaporated and (---) solution-cast PVDF. The inset shows the IR spectra for (1) α , (2) β , (3) $\alpha + \beta$ forms as reported by Murayama, and (4) evaporated PVDF.

identify the form of the PVDF films used in the present investigation, which may also be found useful in interpreting the conduction behavior, as will be discussed later. The IR spectra of solution-cast PVDF films and that of film obtained by evaporation of the powder are reproduced¹³ in Figure 2. The evaporated film is found to contain mainly the α form. However, a few weak absorption peaks corresponding to β form are also evident. The IR spectrum of our sample was compared with the IR spectra for PVDF reported by Murayama and Hashizumi.¹⁴ This is shown in the inset of Figure 2 superimposed with the IR of the evaporated PVDF in the range of 450–550 cm^{-1} . The curves marked 1, 2, and 3 correspond to the spectra for α , β , and $\alpha + \beta$ forms, respectively. Murayama and Hashizumi found two peaks at 520 and 485 cm^{-1} for films containing α form and 500 and 485 cm^{-1} for the films containing β form. For the films possessing both the α and β forms, peaks at 520, 485, and 495 cm^{-1} were displayed. It is evident from the IR spectrum of our films that although they possess α form predominantly; a few weak absorption peaks that correspond to β form could also be seen from the enlarged spectra shown in the inset of Figure 2. During the current-voltage measurements, it was noticed that the current tends to become unstable at higher electric fields (at higher applied voltages) and the

device was found to transform itself to a much higher conduction state than expected. To transform the device again to its original low conduction state, it was found necessary to apply a high voltage (giving field > 60 MV/m) singular pulse of 100 μs . This could be expected to transform the device back to its original high-resistance state by sudden melting and quenching.¹⁵ This aspect is being studied in detail and will be reported elsewhere. In the case of PVDF, it was reported that such cooling at a superhigh rate results in the formation of β -phase crystallites.^{4,5} It is reasonable, therefore, to believe that our films that were subjected to high-field short-duration pulses could also have resulted in possessing partial β phase. Hence, the films used in the study of dc conduction mechanism could be of $\alpha + \beta$ form rather than pure α form. It was, however, not possible to obtain IR spectra on the films owing to thick aluminum contacts deposited on it. It was further observed that the loss tangent of these films showed about 10 times higher values^{13,16} than reported for solution-cast films. According to Yasuda,¹⁷ this could be attributed to the presence of polar groups in the film. It was further suggested by Murayama and Hashizumi that the films having $\alpha + \beta$ form would produce trapping sites. Electrical properties in such a case will therefore be mainly governed by a trapping mechanism.

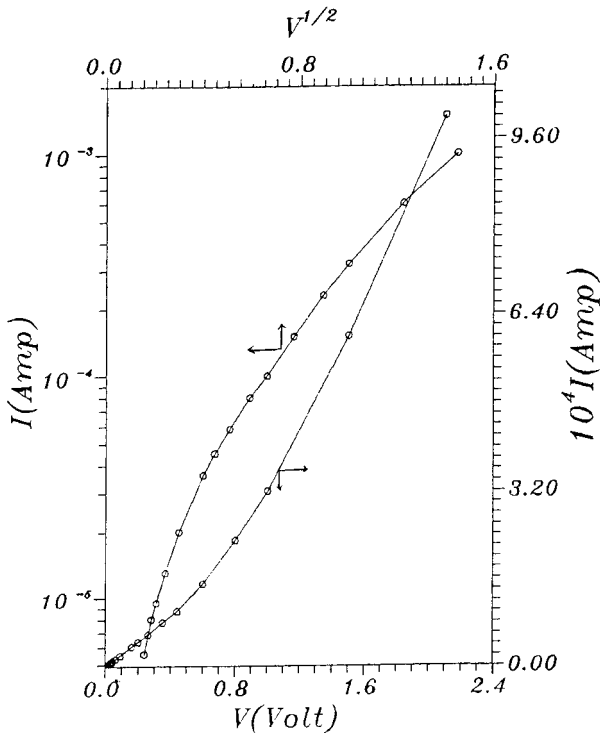


Figure 3 I versus V and $\log I$ versus $V^{1/2}$ curves for PVDF film with a thickness of 90 nm at room temperature.

Figure 3 shows room temperature I - V and $\log I$ - $V^{1/2}$ curves for a typical representative sample with film thickness of 90 nm. The nonlinear I - V curve suggests that the possible conduction mechanism could be Richardson-Schottky (RS), Poole-Frenkel (PF), or space-charge-limited (SCL) conduction. However, a plot of $\log I$ - $V^{1/2}$ is also nonlinear, which rules out the possible existence of the RS- or PF-type conduction mechanisms. The I - V characteristics of Figure 3 are therefore replotted as $\log I$ - $\log V$ for the samples of various film thicknesses and are shown in Figure 4. It is seen that the curve for each thickness, S , shows two distinct regions. At low fields (smaller applied voltages), it shows ohmic behavior, whereas, at high fields, it exhibits square-law dependence. It is also seen from the curves that conductivity increases with the decrease in film thickness. Also, the transition from Ohm's law to square law takes place at voltage, V_{tr} , which decreases as the thickness of the film decreases. The nature of these curves suggests that the conduction be of SCL type. However, to establish the dominant mode of conduction in a particular material, one has to look into the detailed analysis of the I - V data of the material in terms of theoretical con-

siderations available for SCL conduction type of process. If the material has a finite-free carrier density, n_0 , under equilibrium conditions at sufficiently low electric fields, the current density due to these carriers yields an Ohmic conduction given by

$$J = en_0\mu V/S \quad (1)$$

where e is the electronic charge (C), μ is the drift mobility of free carriers ($\text{m}^2/\text{V s}$), V is the applied voltage (V), and S is the thickness (m).

For the current to be space-charge-limited on the high-field region, the current density, J , should obey the Child's law,^{18,19} which gives the equation for J as

$$J = [9\varepsilon\mu V^2]/[8S^3] \quad (2)$$

where ε is the permittivity of the material (F/m).

If the nonlinear response of current to applied voltage is due to the charge injection at the electrode-polymer interface, a large excess carrier density will exist at the injection electrode. This

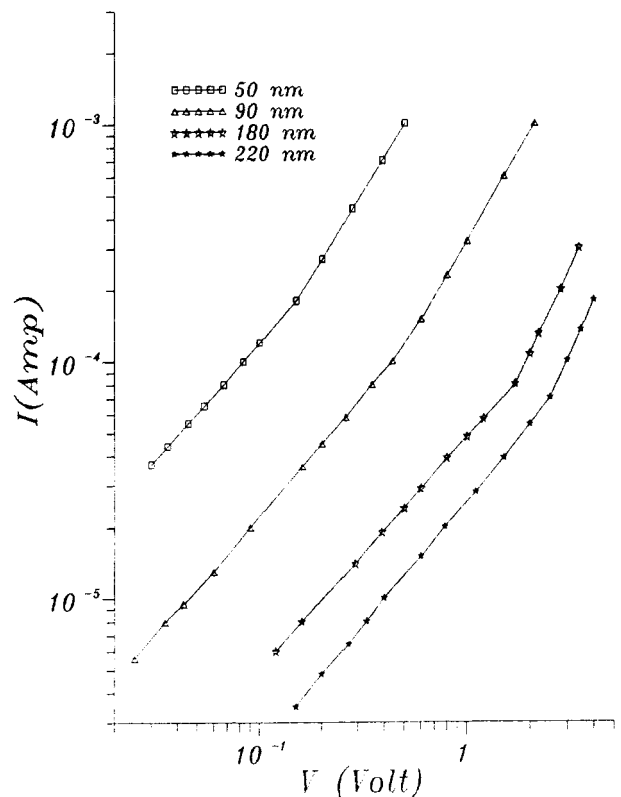


Figure 4 $\log I$ versus $\log V$ plots for PVDF films of various thicknesses at room temperature.

excess carrier density will give rise to the space-charge-limited current flow. A material that may be ohmic at low applied voltages may now follow the quadratic law at a certain voltage V_{tr} . At this voltage, the density of injected charge equals the equilibrium charge density. The expression for this voltage can be found by equating eqs. (1) and (2) at the applied voltage $V = V_{tr}$. Hence,

$$V_{tr} = 8en_0S^2/9\epsilon \quad (3)$$

To further confirm the existence of SCL conduction in light of the above discussion, magnitudes of current I at a particular constant voltage (in square-law region) for various thicknesses are obtained by using the data of Figure 4 and replotted as $\log I$ versus $\log S$ and $\log V_{tr}$ versus $\log S$ as depicted in Figure 5. It is seen that both the curves are linear with slopes -3 and 2 , respectively. This further confirms the existence of SCL conduction in lieu of eqs. (2) and (3), respectively. It is now necessary to evaluate the trap density and its variation with temperature and also to calculate its activation energy. Figure 6 gives the temperature variation of $\log I$ versus $\log V$ curves for the representative sample with a film thickness of 90 nm. It is seen that slopes of the curves in region II are temperature dependent, decreasing slightly with the increase in temperature.

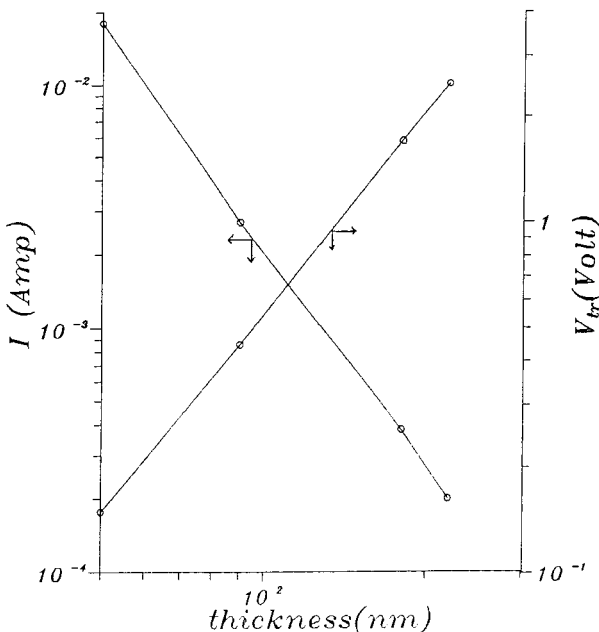


Figure 5 $\log I$ versus thickness and V_{tr} versus thickness plots for PVDF films at room temperature.

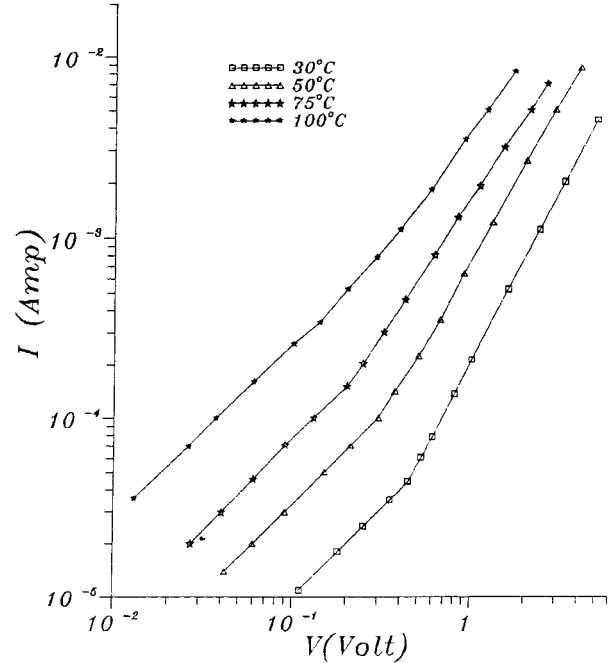


Figure 6 $\log I$ versus $\log V$ curves at various temperatures for PVDF film with a thickness of 90 nm.

When the traps exist in the material, if they are located above the Fermi energy level, E_F (shallow traps), and are in quasi-thermal equilibrium with the free carriers, the form of current density is²⁰

$$J = \theta\epsilon\mu V^2/S^3 \quad (4)$$

and

$$V_{tr} = en_0S^2/\theta\epsilon \quad (5)$$

where

$$\theta = N_c \exp[(E_t - E_c)/KT]/N_t \quad (6)$$

and N_c is the density of states in the conduction band (m^{-3}), N_t is the concentration of traps ($m^{-3} eV^{-1}$), E_t is the energy level of traps (eV), K is the Boltzmann's constant (eV/K), and T is the temperature (K). θ can also be written as

$$\theta = n_0/n_t \quad (7)$$

where n_0 is the free carrier density (m^{-3}) and n_t is the trapped carrier density (m^{-3}). Hence,

$$n_t = V_{tr}\epsilon/eS^2 \quad (8)$$

Thus the decrease in V_{tr} implies the decrease in n_t that will increase the conductivity of the device.

Although the same total charge is forced into the insulator with shallow traps as in the case of trap-free insulator, only a fraction of this charge is free. The drift mobility must then be reduced by the same fraction. The value of this fraction is determined by the number and depth of traps and is not dependent on the applied voltage. Hence, the current density is then given as²¹

$$J = \theta \epsilon \mu' V^2 / S^3 \quad (9)$$

where μ' is the effective drift mobility.

Discrete trap levels may be expected to occur in single crystal materials of a high degree of purity, whereas distributed trap levels may be expected in amorphous and polycrystalline materials and may be related to an intrinsic disorder of the lattice, possibly due to variation in the nearest neighboring distances. This leads to the distribution of states in energy materials deposited by evaporation when perfect crystallinity is unlikely and the density of such defects might be rather high.²²

In amorphous/polycrystalline structures, which are characteristic of thin film dielectrics, a distribution of traps is to be expected rather than a discrete level of traps. Rose (1955)²¹ treated the case of SCL conduction in the presence of a distribution of trap levels that decrease exponentially in density with increasing energy below the conduction band. He considered this dependence as $N_t = A \exp(-E_t/KT_c)$, where A is a constant, E_t is the energy measured from the bottom of the conduction band, and T_c is a characteristic temperature greater than the temperature, T , at which the currents are measured. Hence, the current-voltage dependence is of the form $I \propto V^{(T_c/T)+1}$. Thus, if the distribution of traps is exponential, $I \propto V^n$, where $n > 2$. Rose has further shown that if $T_c > T$ but $KT_c \ll E_t$, the distribution is not exponential but uniform.

In our case, as shown in Figure 4, for all the thicknesses studied in the square-law region, $n < 2$, which indicates that the distribution of traps could not be exponential. Further, for the sample of film thickness 90 nm, $KT_c = 0.026$ eV at room temperature, whereas the activation energy calculated for the same is 0.263 eV. It is therefore evident that the traps are distributed uniformly. Thus, if the traps are distributed uniformly in energy below the conduction band, for given ap-

plied voltage, the charge Q is forced into the insulator. This will give rise to a shift in the Fermi level proportional to the space-charge Q that in turn is proportional to the applied voltage V .

Hence, the thermally generated free-carrier density, n_{co} , will be given by

$$n_{co} = N_c \exp[(E_F - E_c)/KT] \exp(\delta E/KT) \quad (10)$$

where δE is the shift in the position of the Fermi level, and

$$\delta E = VC/(AeN_t S) \quad (11)$$

where C is the capacitance formed by the material sandwiched between the two electrodes (F), and A is the electrode area (m^2). The density of trapped carriers, n_t , in such a case, is given as

$$n_t = Q/AeS = VC/AeS = V\epsilon/eS^2 \quad (12)$$

Now

$$\theta = n_{co}/n_t$$

Hence

$$\theta = en_0 S^2 \exp(VC/AeN_t SKT)/\epsilon V \quad (13)$$

The current density, J , is then given as

$$J = en_0 \mu' V \exp(V\epsilon/eN_t S^2 KT)/S \quad (14)$$

Hence

$$I/V = Ae n_0 \mu' \exp(V/V_0)/S \quad (15)$$

where

$$V_0 = eN_t S^2 KT/\epsilon \quad (16)$$

Hence, by plotting a graph of $\log(I/V)$ versus V , for various thicknesses at room temperature, we get the intercept on $\log(I/V)$ axis as

$$(Ae n_0 \mu' / S) = A_0 \quad (17)$$

and slope as, $1/V_0$, as shown in Figure 7. From the slope, concentration of traps, N_t , was calculated by using eq. (16). The value of the dielectric constant was used as $K = 6.4$ as reported by Tripathi and others²³ and is close to the value

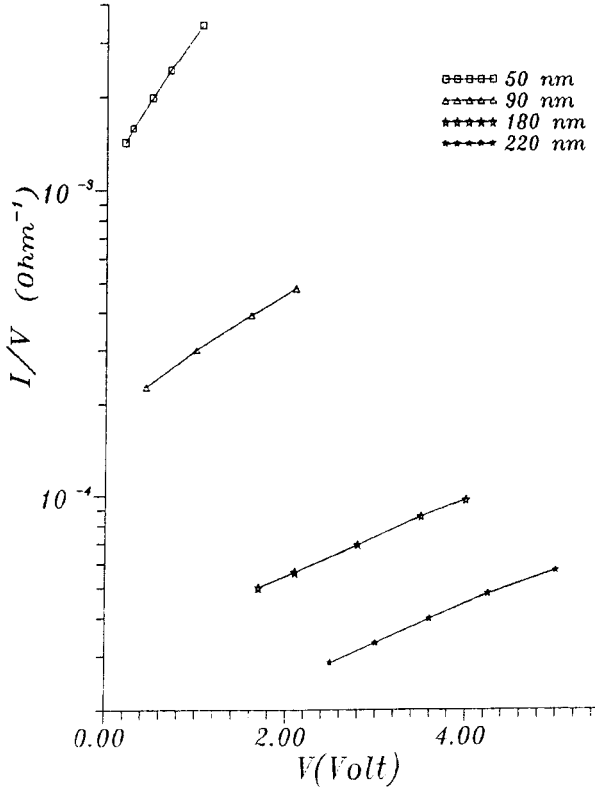


Figure 7 Log(*I/V*) versus *V* plots for PVDF films of various thicknesses at room temperature.

obtained on our samples. For the room temperature, the values of N_t for various film thicknesses are tabulated in Table I. Similarly, by plotting $\log(I/V)$ versus V for given thickness S at different temperatures, the variation of trap density with temperature could be evaluated. Figure 8 gives such plots for a film thickness of 90 nm. The variation of N_t with temperature for a sample thickness of 90 nm is given in Table II.

The mobility of carriers is given as

$$\mu = \mu_0 \exp(-E_t/KT) \tag{18}$$

where E_t is the activation energy. For the conductivity

Table I Variation of N_t with Thickness at Room Temperature

Thickness (nm)	N_t ($m^{-3} eV^{-1}$) ($\times 10^{24}$)
50	2.32
90	1.39
180	0.7
220	0.5

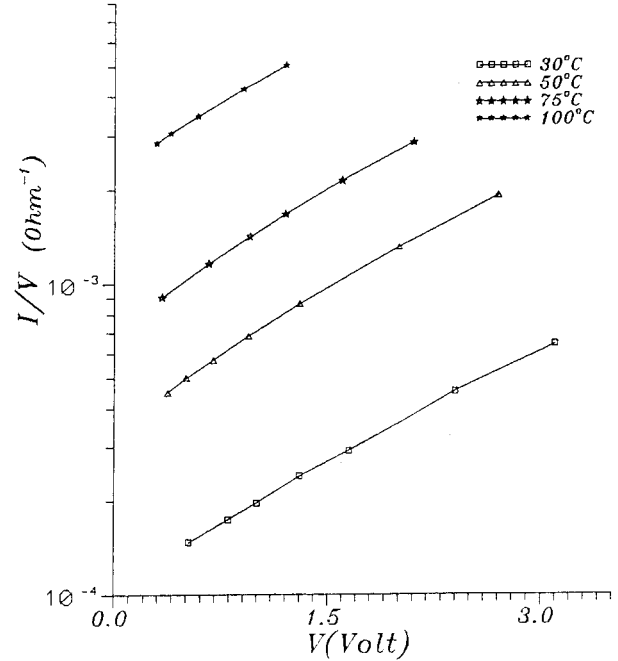


Figure 8 Log(*I/V*) versus *V* plots at various temperatures for PVDF film with a thickness of 90 nm.

$$\sigma = en_0\mu' = en_0\mu'_0 \exp(-E_t/KT) \tag{19}$$

From eq. (17), $n_0\mu' = A_0S/Ae$; hence, $n_0\mu'$ can be calculated at different temperatures for a given thickness from Figure 8. By plotting a graph of $\log(n_0\mu')$ versus $1/KT$ (Fig. 9), the activation energy can be calculated. The activation energy thus calculated for the typical sample is 0.263 eV.

CONCLUSION

Vacuum-evaporated thin films of PVDF at best possess α form. However, application of high-voltage short-duration pulse converts it to mixed $\alpha + \beta$ phase. The conduction process in these films is of space-charge-limited type. The traps, which influence the conduction process, are uniformly

Table II Variation of N_t with Temperature (Film Thickness: 90 nm)

Temperature (K)	N_t ($m^{-3} eV^{-1}$) ($\times 10^{24}$)
303	1.4
323	1.17
348	1.107
373	1.016

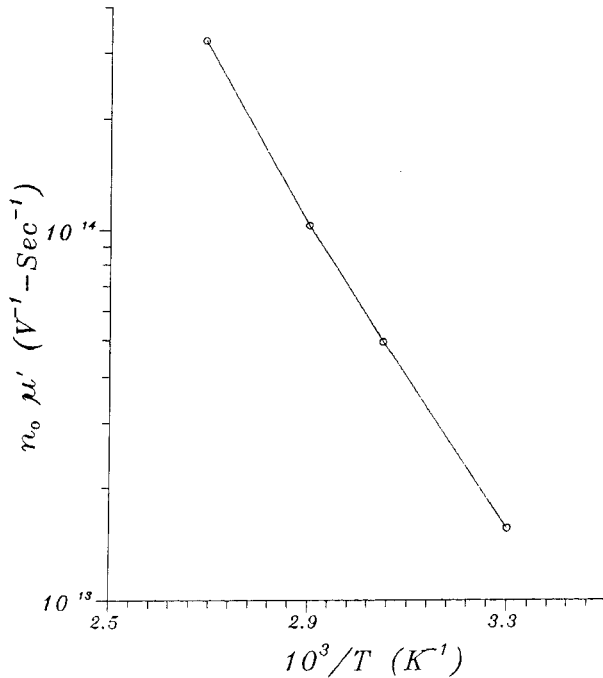


Figure 9 $\text{Log}(n_0\mu')$ versus $1/T$ plot for PVDF film with a thickness of 90 nm.

distributed with an average activation energy of 0.263 eV. The trap density is found to decrease with an increase in film thickness as well as temperature.

REFERENCES

- Sessler, G. M. *J Acoustic Soc Am* 1981, 70, 1596.
- Lu, F. J.; Hsu, S. L. *Polymer* 1984, 25, 1247.
- Sen, A.; Scheinbeim, J. I.; Newman, B. A. *J Appl Phys* 1984, 56, 2433.
- Kepler, R. G.; Anderson, R. A. *CRC Critical Review in Solid State and Materials Sciences*, 399, November 1980.
- Gregorio, R., Jr.; Cestari, M. *J Poly Sci, B Polym Phys Ed* 1994, 32, 859.
- Burkard, M.; Pfister, C. *J Appl Phys* 1974, 45, 3360.
- Sussner, H. *Phys Lett A* 1976, 58, 426.
- Ohigashi, H. *J Appl Phys* 1976, 47, 949.
- Phadke, S. D.; Sithianandan, K.; Karekar, R. N. *Thin Solid Films* 1978, 51, L9.
- Michel, R. E.; Chapman, F. W. *J Poly Sci, Polym Chem Ed* 1970, 8, 1159.
- Gawande, W. G.; Pakade, S. V.; Yawale, S. P.; Motke, S. G.; Burghate, D. K. *J Poly Mater* 1996, 13, 233.
- Christy, R. W. *J Appl Phys* 1964, 35, 2179.
- Bodhane, S. P.; Shirodkar, V. S. *J Appl Polym Sci* 1997, 64, 225.
- Murayama, N.; Hashizumi, H. *J Polym Sci, Polym Phys Ed* 1976, 14, 989.
- Nadkarni, G. S.; Shirodkar, V. S. *Thin Solid Films* 1982, 94, 101.
- Mizutani, T.; Yamada, T.; Ieda, M. *J Phys D: Appl Phys* 1981, 14, 1139.
- Yasuda, H. *Plasma Polymerization*; Academic Press: San Diego, CA, 1985; Chapter 11.2, p 379.
- Brown, J. M.; Jordan, A. G. *J Appl Phys* 1966, 37, 337.
- Simmon, J. G. *J Phys D: Appl Phys* 1971, 4, 613.
- Caserta, G.; Rispoli, B.; Serra, A. *Phys Status Solid* 1969, 35(1), 237.
- Rose, A. *Phys Rev* 1955, 97, 1538.
- Sussman, A. *J Appl Phys* 1967, 38, 2738.
- Tripathi, A.; Tripathi, A. K.; Pillai, J. *Mater Sci Lett* 1992, 11(24), 1647.